Scanning Microscopy

Volume 8 | Number 4 Article 6

12-12-1994

Recent Surface Studies Using Biassed Secondary Electron Imaging

Rajendra Persaud
The State University of New Jersey

Hisato Noro
NKK Corporation

Muhammad Azim
University of Sussex

Robert H. Milne
University of Sussex

John A. Venables
Arizona State University

Scanning Microscopy, Vol. 8, No. 4, 1994 (Pages 803-812) 0891-7035/94$5.00+.25
Scanning Microscopy International, Chicago (AMF O'Hare), IL 60666 USA

RECENT SURFACE STUDIES USING BIASSED SECONDARY ELECTRON IMAGING

Rajendra Persaud[1], Hisato Noro[2], Muhammad Azim, Robert H. Milne and John A. Venables[3,*]

School of Mathematical and Physical Sciences, University of Sussex, Brighton BN1 9QH, United Kingdom
[1]Now at Serin Physics Lab., Rutgers, The State University of New Jersey, Piscataway, NJ, 08855-0849, U.S.A.
[2]Permanent address: R & D Division, NKK corporation, Kawasaki 210, Japan
[3]also at Department of Physics and Astronomy, Arizona State University, Tempe, AZ 85287, U.S.A.

(Received for publication June 14, 1994 and in revised form December 12, 1994)

Abstract

The growth and surface diffusion of Cs on Si(100) and Ag on Fe(110) have been studied using biassed secondary electron imaging (b-SEI) and Auger electron spectroscopy (AES).

The b-SEI technique was found capable of detecting Cs on the Si surface with a 0.5% ML sensitivity. Unusual diffusion profiles containing linear sections were obtained for coverages (θ) < 1/2 ML. The general form of these profiles were reproduced using a 2-phase model, where Cs chains act as sources of mobile adatoms, in conjunction with a diffusion coefficient of the form $D \sim \theta (1 - C\theta)$. This form of D, obtained from Boltzmann-Matano analysis, is consistent with diffusion theory including strongly repulsive Cs-Cs interactions. An adatom diffusion energy, E_d, = 0.47 ± 0.05 eV was found to be consistent with measurements of the diffusion coefficient made in the temperature range $333 \leq T \leq 363$K.

The growth mode for Ag on Fe(110) was determined by AES and b-SEI to be Stranski-Krastanov, with islands growing on top of two intermediate layers. Diffusion experiments conducted on finite Ag patches show that following annealing, adatoms dissociate from the islands and second monolayer and contribute to the observed expansion of the first monolayer. The diffusion results also indicate that while islands are still present, there is a competition between adatoms entering and leaving the second monolayer.

Key Words: Caesium on silicon, Stranski-Krastanov growth, silver on iron, surface diffusion, biassed secondary electron imaging.

*Address for correspondence:
John A. Venables
School of Mathematical and Physical Sciences,
University of Sussex,
Brighton BN1 9QH, U.K.
Telephone number: (44) 1273 678077
FAX number: (44) 1273 678097

Introduction

Over the last six decades, alkali-metal (AM) adsorption systems have been the subject of many scientific studies (Taylor and Langmuir, 1933; Soukiassian *et al.*, 1992). The motivation behind such studies is two-fold. From the perspective of fundamental physics, they are amongst the most simple of chemisorption systems and should allow for accurate computations of their electronic structures. From an industrial viewpoint, the dramatic reduction in the work function induced by AM adsorption, enhances the emission properties of the substrate, leading to applications as highly efficient thermionic emitters and photocathodes. Alkali-metals are also useful as catalysts to enhance the oxidation of semi-conductor substrates. In spite of the extensive research on these systems, including Cs/Si(100) (Papageorgopoulos and Kamaratos, 1989), there are still many unresolved questions regarding the overlayer structure and nature of the AM-substrate bonding.

In comparison to Cs/Si(100), there have been few studies of the Ag/Fe(110) system. It is, however, an attractive system for studying the processes involved in nucleation and growth, as complexities associated with alloying and inter-diffusion are avoided. A proper characterization of this interface is also instructive in connection with the technologically important magnetic multi-layer (Fe/Ag/Fe) sandwiches.

In this paper, we present results from biassed secondary electron imaging (b-SEI) studies of the diffusion of Cs on Si(100)2x1 and Ag on Fe(110). The b-SEI technique was also used in conjunction with Auger electron spectroscopy (AES) to establish the growth mode for Ag on Fe(110). These studies are useful for extracting the atomic energies controlling nucleation, growth and diffusion processes (Venables, 1994).

Experimental Details

The experiments were conducted using an ultra high vacuum-scanning electron microscope (UHV-SEM) which has been previously described (Futamoto *et al.*,

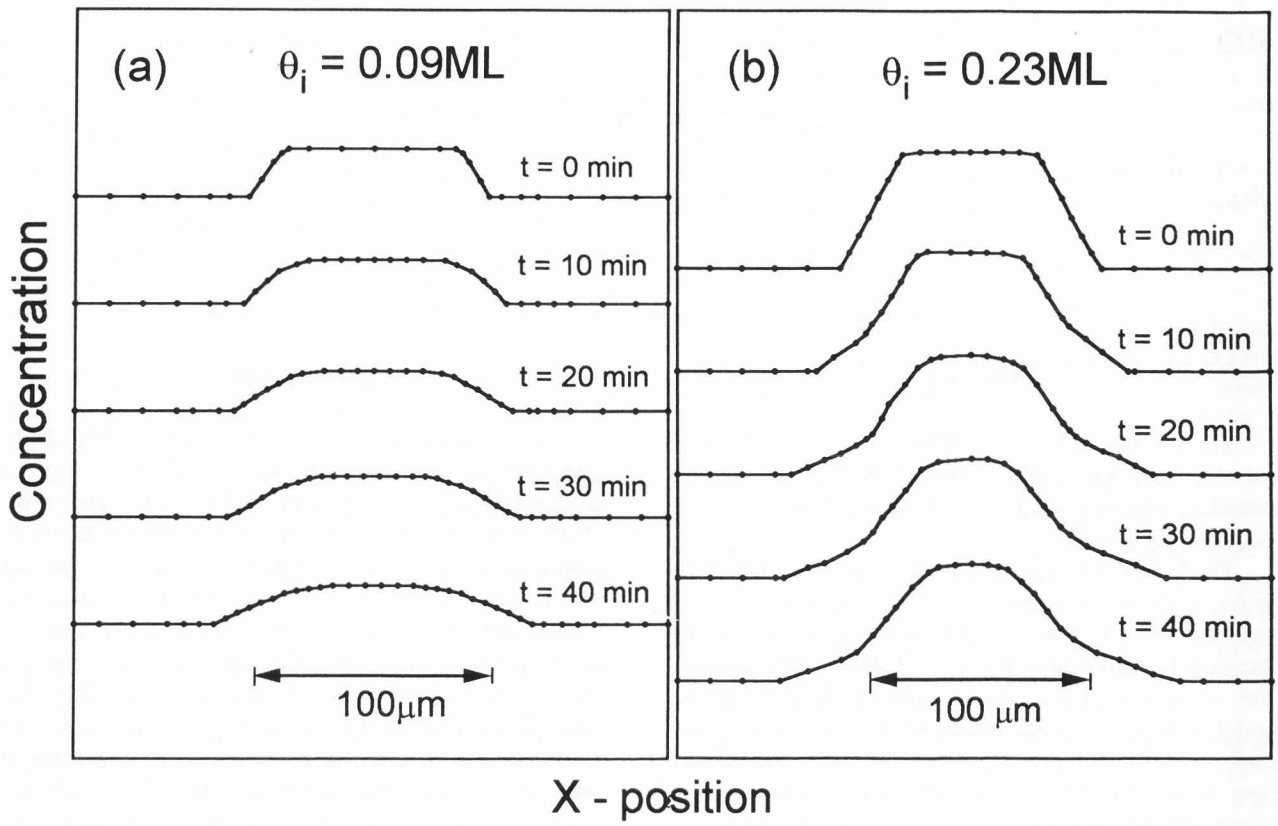

Figure 1. Examples of diffusion profiles obtained for Cs/Si(100): (**a**) θ_i < 1/6 ML and (**b**) θ_i > 1/6 ML. Anneal temperature, 333K. Values of θ_i given on the figures correspond to the maximum concentration and establish the vertical scale. Each profile was measured in 5 seconds. The secondary electron signal was converted to produce the concentration profiles (Azim *et al.*, 1993).

1985; Harland *et al.*, 1987). For the SEM studies, a field emission gun served as the electron source and secondary electrons were collected using a conventional Everhart-Thornley detector. The system is placed in the b-SEI mode by applying a negative bias to the sample. For Cs/Si(100) the maximum contrast was obtained with the sample biassed at -600 volts, whereas for Ag/Fe(110) the corresponding value was ~-100V. The UHV chamber was also equipped with a cylindrical mirror analyzer (CMA) for AES, and a reflection high energy electron diffraction (RHEED) system for determining surface crystallography.

The Si samples (p-type, ρ = 7 - 13 Ω.cm, size 22 mm x 5 mm) used in the Cs/Si(100) experiments were cleaned through resistive heating up to 1420K in a background pressure of ~4 x 10^{-10} torr. Temperatures were measured using an optical pyrometer and, at lower temperatures, an infra-red pyrometer calibrated to an Alumel-Chromel thermocouple. Cs was deposited at a rate of 0.1 monolayer (ML)/min by passing a direct current though a commercially available SAES alkali-metal getter dispenser. For Cs/Si(100), 1 ML is defined as 6.78 x 10^{14} atoms/cm^2. The coverage was determined by calibrating the secondary electron contrast with the work function versus coverage curve (Azim *et al.*, 1993a,b). Due to the large decrease in work function, Cs concentrations were detected with a sensitivity of around 0.5% ML using b-SEI.

For the Ag/Fe(110) studies, a water-cooled Knudsen source, calibrated using a quartz crystal microbalance, was used to deposit silver at a rate of 0.4-0.5 ML/min. With regard to the Ag/Fe(110) system, 1 ML is defined as the areal density of Ag(111) = 1.38 X 10^{15} atoms/cm^2. A 7 mm diameter Fe(110) single crystal disc (purity 99.94 wt%), polished up to 0.25 μm diameter diamond paste, was used in these studies. Temperature measurements were made with a W-3%Re - W-25%Re thermocouple. The sample was heated through a combination of radiation and electron bombardment from a tungsten filament mounted behind the sample. Initial sample contamination was removed after several iterations of argon ion (Ar^+) bombardment at 870K,

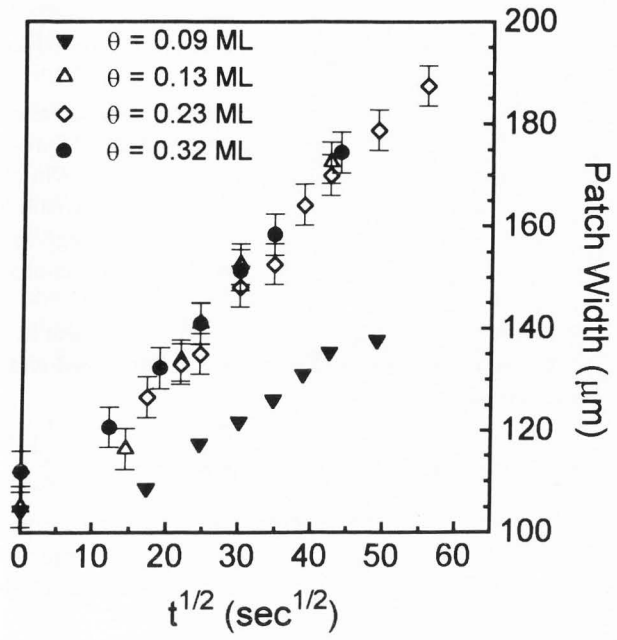

Figure 2. The expansion of the Cs patches as a function of the square root of time for annealing at 333K; $\Delta x \sim 1$ μm, $\Delta t \sim 5$ seconds. The slopes are essentially invariant for $1/6 < \theta_i < 1/3$ ML, but different otherwise (lower curve).

---

followed by annealing in the presence of oxygen under *in situ* RHEED observations. After this initial procedure it was sufficient to use Ar^+ bombardment followed by flashing to 870K to recover a clean surface.

Diffusion experiments in both cases were conducted using finite patches, produced by depositing through a perforated mask {holes ~100 μm x 100 μm (Cs), 20 μm x 100 μm (Ag)} positioned in front of the sample.

Results and Discussion

Cs/Si(100)

While some aspects of AM adsorption remain controversial, it is generally agreed that at low coverages, electron transfer between the adatoms and substrate results in the formation of dipoles, leading to a dramatic decrease in the work function of the substrate (Lang, 1971). As the coverage increases, each dipole is subject to a depolarization arising from the electric field due to all the others. The work function versus coverage curve goes through a minimum when the increase in number of dipoles is balanced by depolarization. Recent experimental studies on Cs/Si(100)2x1 indicate that Cs adatoms occupy pedestal sites up to a coverage of $\theta = 1/2$ ML. Thereafter, the adatoms occupy cave sites which have a much reduced adsorption energy, until saturation (Abukawa and Kono, 1989). It is believed that the saturation coverage at room temperature (RT) is 1 ML whereas the minimum in the work function curve corresponds to 1/2 ML (Ortega *et al.*, 1987). This double layer model has been theoretically supported by Zhang *et al.* (1991) and Kobayashi *et al.* (1992).

In the current experiments, patches of Cs with initial concentration (θ_i) ranging from 0.09 to 0.44 ML, were deposited on the Si surface at RT and subsequently annealed to accelerate the diffusion process. As exemplified in Figure 1a, for $\theta_i < 1/6$ ML, the diffusion profiles show an almost linear concentration gradient at the edges of the patch. For $\theta_i > 1/6$ ML (Figure 1b), the linear components of the profiles are still observed, but are generally in the regions below 1/12 ML.

The expansion of the patches varied linearly with the square root of annealing time over the entire coverage range studied. However, as shown in Figure 2, for $1/6 < \theta_i < 1/3$ ML, the slopes of these lines are essentially invariant. This suggests that the diffusion coefficient, D, is independent of θ_i in this region. Here we offer a qualitative and quantitative explanation for the peculiarities in the profiles and for the anomalous behaviour of the diffusion coefficient.

Low energy electron diffraction (LEED) studies on Cs/Si(100)2x1 show the presence of a stable structure at $\theta = 1/6$ ML where every third pedestal site is occupied (Abukawa *et al.*, 1991). No ordered structures were observed below this coverage at RT. The next stable structure probably consists of pairs of atoms separated by one unoccupied site, corresponding to $\theta = 1/3$ ML. Using these considerations, our experimental results can be explained in terms of 2-phases: 1) a condensed phase, where chains of two or more adjacent atoms act as sources of adatoms, and 2) a dilute phase of atoms separated by at least 2 unoccupied sites, which dominates the diffusion. In terms of the general theory of alkali-metal adsorption outlined earlier, it is assumed that there will be dipole-dipole repulsion between the individual atoms in the dilute phase. However, at higher coverages, adatoms in adjacent sites will experience diminished repulsion due to increased depolarization and bonding between the adatoms. Above $\theta = 1/3$ ML, the rate limiting steps for diffusion are the dissociation of chains in the condensed phase and the number of available sites.

A general form of the diffusion coefficient necessary to produce a linear concentration profile can be obtained from the Boltzmann-Matano equation

$$D(\theta) = -\frac{1}{2t}\left(\frac{dx}{d\theta'}\right)_{\theta}\int_0^{\theta} x\, d\theta' \qquad [1]$$

where t is the annealing time and x the distance from the

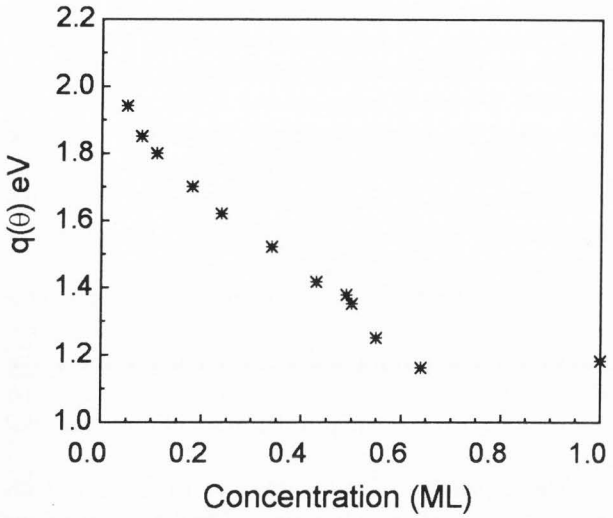

Figure 3. The dependence of the heat of adsorption $q(\theta)$ on coverage for Cs on Si(100).

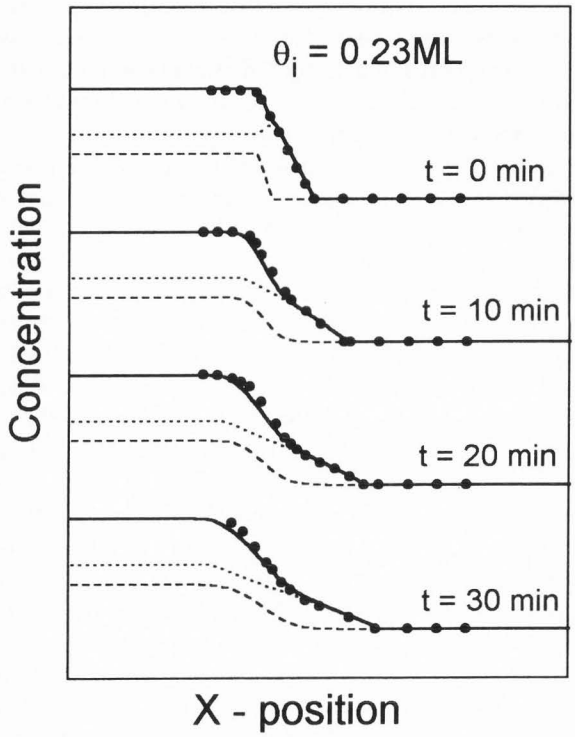

Figure 4. Comparison between Cs diffusion profiles obtained experimentally (solid circles) and numerically generated (solid line) using model described in the text. The upper dotted curve is the concentration of the dilute phase and the lower, the condensed phase. See text for details.

---

initial step in the concentration profile. Assuming an initial step profile evolves to give a linear concentration gradient and that the edges expand as $\Delta x = (2D_e t)^{1/2}$ (as in our results), equation [1] yields

$$D(\theta) = \frac{D_e}{\theta_1}[\theta(1-C\theta)] \qquad [2]$$

here θ_1 is half the initial concentration, C a constant and D_e, an effective diffusion constant. Equation [2] predicts that single isolated adatoms will not diffuse. While this is of course incorrect, a more general thermodynamic argument, outlined below, shows that the form given by equation [2], dominates when repulsive interactions are considered.

A more general form of the diffusion coefficient including lateral interactions has been given by Reed and Ehrlich (1981) as

$$D(\theta) = \Gamma(\theta)\lambda^2 \frac{\partial(\mu/kT)}{\partial \ln\theta} \qquad [3]$$

where μ is the chemical potential, k Boltzmann's constant, $\Gamma(\theta)$ the adatom jump frequency and λ, the jump distance. For interacting atoms, the chemical potential is given by

$$\mu = \mu^0 + kT\ln\left(\frac{\theta}{1-\theta}\right) - q(\theta) \qquad [4]$$

where μ^o is the standard chemical potential and $q(\theta)$ is the heat of adsorption. Our experimental results showing the variation of the heat of adsorption with coverage are presented in Figure 3. As in the case for Na/Si(001)2x1 (Tikhov *et al.*, 1991), the curve is essentially linear at low coverages. It is therefore quite reasonable, at low coverage, to express it as

$$q(\theta) = q_o - A\theta \qquad [5]$$

where A is the slope. If the semi-empirical formalism used by Reed and Ehrlich (1981) is adopted, then $\Gamma(\theta)$ can be written as

$$\Gamma(\theta) = \nu(1-\theta)\exp\left[\left(\frac{\partial \ln\theta}{\partial\mu}\right)_T\left(\frac{\partial(-q(\theta))}{\partial\ln\theta}\right)_T\right]\exp\left(-\frac{E_d}{kT}\right) \qquad [6]$$

at low coverages. The first exponential term accounts for the effects of the repulsive interactions on the barrier to diffusion, ν is an attempt frequency and E_d, the adatom diffusion energy. Using equations [3-6] the following expression is obtained for $D(\theta)$:

$$D(\theta) = \nu\lambda^2\left[1 + \frac{A\theta(1-\theta)}{kT}\right]\exp\left[\frac{A\theta(1-\theta)}{kT + A\theta(1-\theta)}\right]\exp\left(-\frac{E_d}{kT}\right) \qquad [7]$$

In the limit $\theta \to 0$, or A = 0 (constant heat of adsorption), equation [7] reduces to the expression for the single adatom diffusion coefficient. As the coverage increases, the term in the first square bracket increases

much more rapidly than the θ dependent exponential and $A\theta(1-\theta)/kT >> 1$. This means that, in essence, equation [7] approximates the Boltzman Matano form (equation [2]). Using $\nu = 10^{13}$ Hz, $\lambda = 3.8 \times 10^{-10}$ m and A = 2 eV/ML, the values of $D(\theta)$ for $\theta < 1/12$ ML obtained from equation [7] match the values obtained from Boltzmann-Matano analysis of the experimental results for the annealing temperatures of 333, 348 and 363K. A good fit is achieved if a value of $E_d = 0.47$ eV is chosen for the Cs diffusion energy. Changing the value of $(\nu\lambda^2)$ by a factor of 5 results in a $\pm$ 0.05 eV change in E_d.

This form of the diffusion coefficient can be used in conjunction with the principles of the 2-phase model to formulate the set of coupled diffusion equations given below.

$$\frac{\partial\theta_d}{\partial t} = \frac{\theta_c N_a}{\tau_{cd}} - \frac{\theta_d N_a}{\tau_{dc}} + \frac{\partial}{\partial x}\left(D_d(\theta_d,N_a,T)\frac{\partial\theta_d}{\partial x}\right) \qquad [8]$$

$$\frac{\partial\theta_c}{\partial t} = \frac{\theta_d N_a}{\tau_{dc}} - \frac{\theta_c N_a}{\tau_{cd}} + \frac{\partial}{\partial x}\left(D_c\frac{\partial\theta_c}{\partial x}\right) \qquad [9]$$

The coupling of the equations stems from the fact that chains present in the condensed phase dissociate to produce adatoms for the dilute phase which can subsequently diffuse. In equations [8] and [9], N_a is the number of available surface sites and θ_c,θ_d, the concentrations of the condensed and dilute phases, respectively. The parameters τ_{cd} and τ_{dc} are the times required for adatoms to move from the condensed to the dilute phase and vice versa. $D_d(\theta_d,N_a,T)$ is of the form given by equation [7] with A = 2 eV/ML (extracted from Figure 3) and $D_0 = \nu\lambda^2$, left as a free parameter. Since the fraction of the condensed phase existing below $\theta = 1/6$ ML is very small, there is essentially no source of adatoms in this regime. In this case, the experimental concentration profiles can be generated using only one equation (eqn. [8]), with the single parameter D_0; all profiles were best fit with $D_0 = 0.1$ cm^2 sec^{-1}. Both equations could also be used in the low coverage region providing τ_{dc} is long enough to prevent any appreciable build up of θ_c within the time range of the experiments (typically 40 minutes). It was possible (and necessary for $\theta_i > 0.32$ ML) to maintain the relationship $\tau_{dc} = 4\tau_{cd}$ over the entire coverage range studied. With D_0 fixed, this means that there are effectively two free parameters, D_c and τ_{dc} (or τ_{cd}). D_c, which was found to decrease with increasing θ_i, allows for some diffusion within the condensed phase. This model was extremely successful in reproducing the features of the experimental diffusion profiles over the entire coverage regime studied. The case for $\theta_i = 0.23$ ML, reproduced using $\tau_{dc} = 200$ minutes and $D_c = 9 \times 10^{-11}$ cm^2 sec^{-1}, is shown in Figure 4. It is interesting to note that although the physics involved in the Cs/Si(100) system is very different from the Ag/Ge(111) case, they are mathematically rather similar, in that both involve diffusion in the presence of two phases (Venables *et al.*, 1993, 1994).

Ag/Fe(110)

Due to the high supersaturation of deposited atoms, the real growth processes are often determined by kinetics rather than thermodynamics (Bauer and van der Merwe, 1986; Venables, 1994). Qiu *et al.* (1992) reported a Frank van der Merwe (FM or layer-by-layer) growth mode for the Ag/Fe(110) system. A simple consideration of the surface energies of the deposit and the substrate {~1.3 and ~2.9 J/m^2, respectively (Bauer and van der Merwe, 1986)} may support this mode. However, the interface has the Nishiyama-Wassermann orientational relationship as in the case of Fe/Ag(111) (Snyman and Olsen, 1973), and the lattice mismatch of ~20% along <110> of the Fe substrate is much too large to avoid the introduction of misfit dislocations. This would, in principle, terminate the FM mode and lead to Stranski-Krastanov (SK) growth.

The Ag and Fe Auger intensities, obtained for deposition at RT and 570K, are shown as a function of Ag coverage in Figure 5. For RT deposition, the Auger curves show linear sections at least up to a coverage of 3 ML, whereas for deposition at 570K, only two linear sections followed by an abrupt reduction of slope at ~2 ML, are observed. This behaviour indicates that this system, similar to Ag/W(110) (Jones *et al.*, 1990), follows the SK mode with three dimensional (3D) islands growing on top of two stable intermediate monolayers. At room temperature, the system appears to follow a quasi-FM growth mode because of high supersaturation, but quantitatively this is incorrect.

Least squares lines, fitted to the two linear sections of the Ag curve, intersected at around 0.8 ML. This indicates that the first monolayer is completed at a coverage of 0.8 ML, a result which is consistent with the c(5X1) structure derived from RHEED data (Noro *et al.*, 1994). An Auger layer growth calculation was performed using the known analyser geometry and the known mean free path for Ag (8.2 Å). The results, plotted as solid lines in Figure 5, clearly show a departure from layer growth after completion of the second monolayer, for deposition at both temperatures.

A series of biassed secondary electron images of Ag patches taken after depositing a 6 ML patch at RT and subsequently annealing at 580K are shown in Figure 6. The viewing angle of ~10° to the surface plane, used

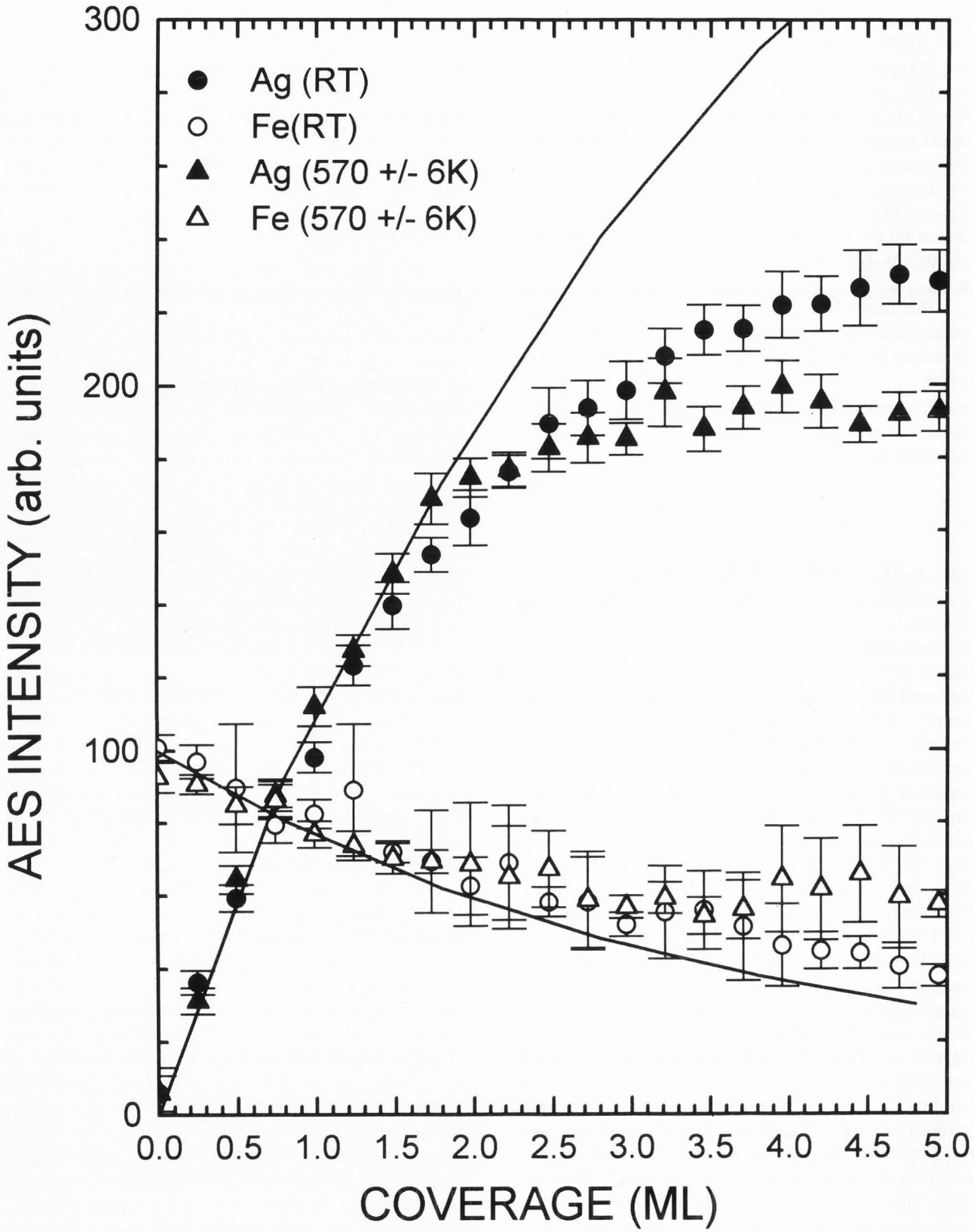

Figure 5. Auger intensities of Ag and Fe as a function of Ag coverage for deposition at room temperature and 570K. The solid lines are obtained from an Auger layer growth calculation using the Ag and Fe mean free paths (8.2 and 8.0 Å, respectively) with the first monolayer completed at 0.8 ML.

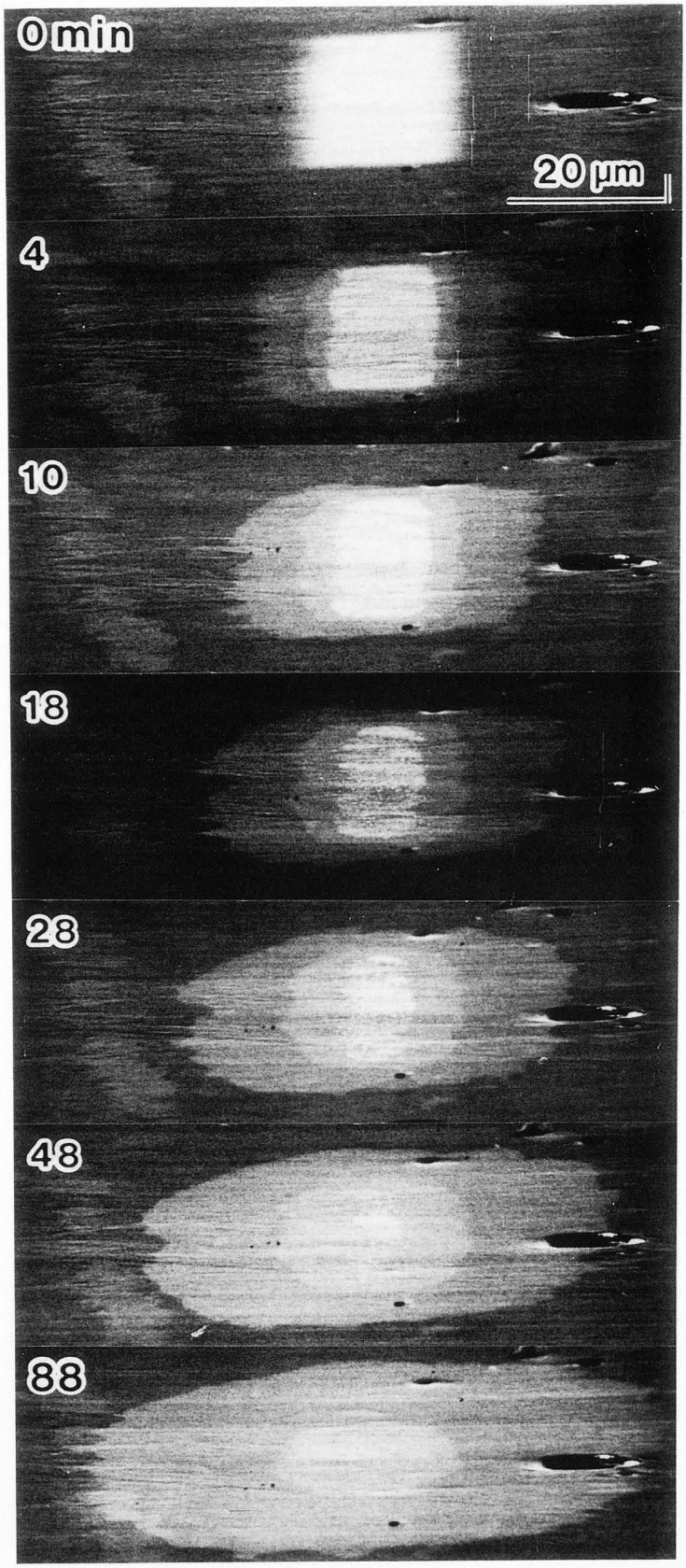

Figure 6. Biassed secondary electron images of 6 ML Ag patches on Fe(110) taken after deposition at room temperature and after successive stages of annealing at 580K.

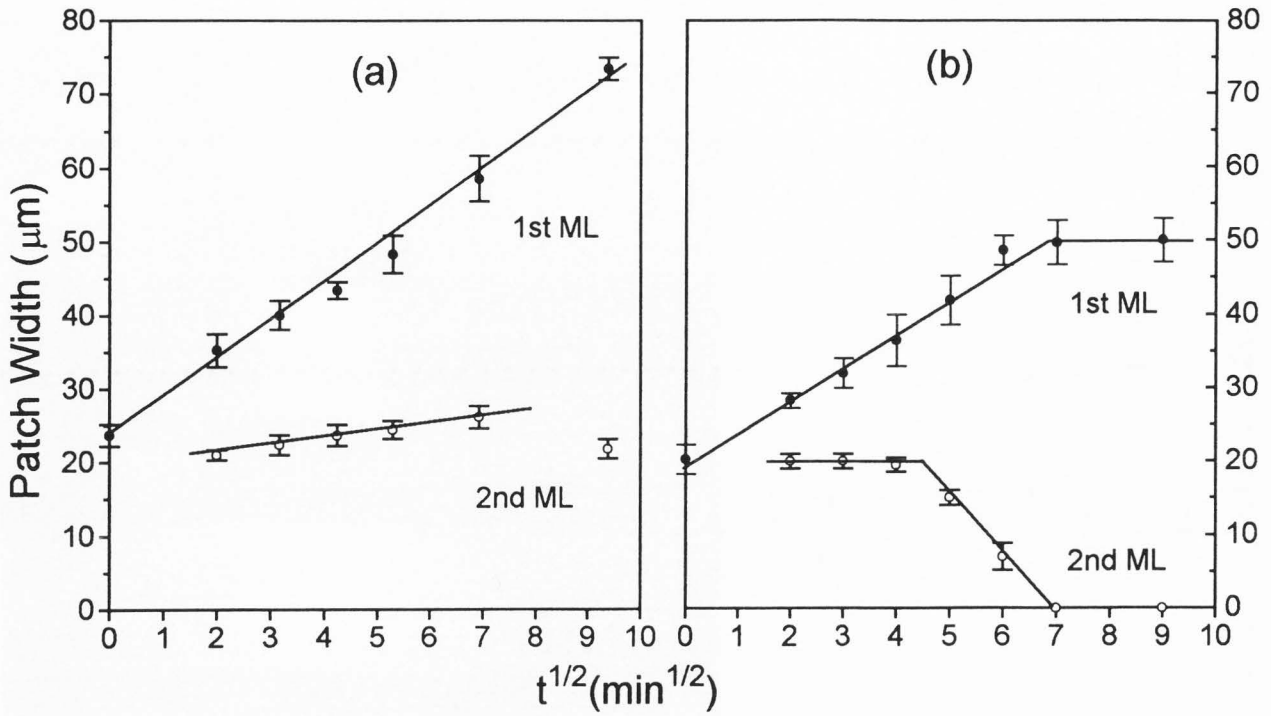

Figure 7. Expansion of (**a**) 6 ML and (**b**) 3 ML Ag patches on Fe(110) as a function of the square root of time. Anneal temperature, 590K.

---

to enhance the secondary electron yield, results in a foreshortening along the long side of the patch. Once annealing starts, the patches split into the two intermediate ML with the 3D islands on top of them appearing as a bright layer at the magnification used. Similar splittings were observed when patches were deposited at elevated temperatures. This clearly supports the Auger data. The islands observed were very thin, with flat surfaces, and their number density varied from 1 x 10^9 to 2 x 10^7 cm^{-2} in the deposition temperature range 450 to 660K. The room temperature behaviour observed in the AES measurements and b-SEI images, is explicable as an increase in the number density of the flat islands.

Upon further annealing, the number of small islands decreases and the first ML spreads simultaneously. The second ML also expands slowly, but starts to shrink rapidly after the disappearance of the islands. The expansion of the first ML continues until the second ML has disappeared, thereafter maintaining its final shape irrespective of annealing. These observations are reflected in Figure 7 which shows the expansion of 6 (Fig. 7a) and 3 ML (Fig. 7b) patches as a function of the square root of the annealing time. In contrast to the 6 ML case, the width of the second ML of the 3 ML deposit remains constant up to a certain annealing time before rapidly decreasing after the disappearance of the islands. These results suggest that the expansion of the first ML is due to surface diffusion of adatoms produced by dissociation of the islands and the second ML. The results obtained for the case of the 3 ML deposit indicate a balance between the dissociation of the second ML and its growth due to the capture of adatoms provided by the islands. It should also be noted that the final width of the first ML remains constant at least up to 610K. This means that re-evaporation is not an important surface process, and that the first ML is essentially stable in this temperature regime. Another interesting feature in Figure 7 is that there is no great slope change for the first ML, even after the disappearance of the islands. Detailed measurements of the effective diffusion coefficients at different annealing temperatures, and the development of a suitable diffusion model to explain the results will be published elsewhere.

Summary

The b-SEI technique was capable of detecting Cs concentrations on Si with a 0.5% ML sensitivity. Unusual diffusion profiles containing linear sections were obtained for θ_i < 1/2 ML. The diffusion coefficient

was found to be independent of coverage for $1/6 < \theta_i < 1/3$ ML. These observations are explained in terms of a 2-phase model where a condensed phase act as a source of adatoms for a dilute phase which dominates the diffusion. The general form of the experimental profiles are reproduced using coupled diffusion equations. The form of $D(\theta)$, obtained from Boltzmann-Matano analysis, is consistent with diffusion theory including strongly repulsive Cs-Cs interactions. An adatom diffusion energy $E_d = 0.47 \pm 0.05$ eV was consistent with measurements of D made in the temperature range $333 < T < 363$K.

In the case of Ag/Fe(110), b-SEI and AES studies show the growth mode of Ag on Fe(110) to be Stranski-Krastanov, with Ag islands growing on top of two stable intermediate Ag layers. For room temperature deposition, Ag appears to grow in a quasi-layer by layer manner, because of high supersaturation. However, an Auger layer growth calculation clearly demonstrates the departure from layer growth after the completion of the second monolayer.

Diffusion experiments performed using patches of Ag on the surface indicate that the first ML expands via surface diffusion of adatoms produced by the dissociation of the islands and second ML. The initial expansion of the first ML shows a $t^{1/2}$ dependence. A competition between the dissociation of the second ML and its growth due to the capture of adatoms provided by the islands is also observed.

Acknowledgements

We thank SERC for funding the experimental work at Sussex. R. Persaud thanks the Natural Sciences and Engineering council of Canada (NSERC) for a post-doctoral fellowship. H. Noro was funded by the NKK corporation and M. Azim by the Government of the Islamic Republic of Pakistan during their stay at the University of Sussex.

References

Abukawa T, Kono S (1989) Photoelectron diffraction and low energy electron diffraction studies of Cs, K/Si(001) surfaces. Surf. Sci. **214**, 141-148.

Abukawa T, Okane T, Kono S (1991) Low energy electron diffraction and X-ray photoelectron diffraction study of the Cs/Si(001) surface: dependence on Cs coverage. Surf. Sci. **256**, 370-378.

Azim M, Milne RH, Persaud R, Venables JA (1993a) Biassed secondary electron imaging of Cs/Si(100). Inst. Phys. Conf. **138**, 197-200.

Azim M, Harland CJ, Martin TJ, Milne RH, Venables JA (1993b) Caesium on Si(100) studied by biassed secondary electron microscopy. Scanning Microsc. **7**, 1153-1160.

Bauer E, van der Merwe JH (1986) Structure and growth of crystalline superlattices: from monolayer to superlattice. Phys. Rev. B **33**, 3657-3671.

Futamoto M, Hanbucken M, Harland CJ, Jones GW, Venables JA (1985) Visualization of sub-monolayers and surface topography by biassed secondary electron imaging: applications to Ag layers on Si and W surfaces. Surf. Sci. **150**, 430-450.

Harland CJ, Jones GW, Doust T, Venables JA (1987) Scanning electron microscopic observations of monolayer deposits using biassed secondary electron and specimen current imaging. Scanning Microscopy Suppl. **1**, 109-114.

Jones GW, Marcano JM, Norskov JK, Venables JA (1990) Energies controlling nucleation and growth processes: the case of Ag/W(110). Phys. Rev. Lett. **65**, 3317-3320

Kobayashi K, Morikawa Y, Terakura K, Blügel S (1992) Optimized structures and electronic properties of alkali-metal (Na,K)-adsorbed Si(001) surfaces. Phys Rev B **45**, 3469-3484

Lang ND (1971) Theory of work-function changes induced by alkali adsorption. Phys. Rev. B **4**, 4234-4245

Noro H, Persaud R, Venables J.A. (1994) The growth and diffusion of Ag on Fe(110). Vacuum, in press.

Ortega JE, Oellig EM, Ferrón J, Miranda R (1987) Cs and O adsorption on Si(100)2x1: A model system for promoted oxidation of semiconductors. Phys. Rev. B **36**, 6213-6216.

Papageorgopoulos CA, Kamaratos M (1989) Adsorption of Cs and its effects on the oxidation of the Ar^+ sputtered Si(100)2x1 substrate. Surf. Sci. **221**, 263-276.

Qiu ZQ, Pearson J, Bader SD (1992) Additivity of the magneto optic Kerr signal in ultrathin Fe(110)/Ag(111) superlattices. Phys. Rev. B **45**, 7211-7216.

Reed DA, Ehrlich G (1981) Surface diffusion, atomic jump rates and thermodynamics. Surf. Sci. **102**, 588 -609.

Soukiassian P, Kim ST, Hurych Z, Rubby JA (1992) Structural properties of Alkali metal/Si(100) 2x1 interfaces investigated by PEXAFS and STM. App. Surf. Sci. **58-58**, 394-401.

Snyman HC, Olsen GH (1973) Application of electron-transparent (111) silver platelets as substrates in epitaxial studies. J. Appl. Phys. **44**, 889-891.

Taylor JB, Langmuir I (1933) The evaporation of atoms, ions and electrons from caesium films on tungsten. Phys. Rev. **44**, 423-458.

Tikhov M, Boishin G, Surnev L (1991) Sodium adsorption on a Si(001)2x1 surface. Surf. Sci. **241**, 103-

110.

Venables JA (1994) Atomic processes in crystal growth. Surf. Sci. **299/300**, 798-817.

Venables JA, Persaud R, Metcalfe FL, Milne RH, Azim M (1993) Coupled Diffusion Equation Solutions to Ag/Ge(111) and Cs/Si(100) interactions. Proc. Mat. Res. Soc. **317**, 83-86.

Venables JA, Persaud R, Metcalfe FL, Milne RH, Azim M (1994) Rate and Diffusion Analyses of Surface Processes. J. Phys. Chem. Solids **55**, 955-964.

Zhang BL, Chan CT, Ho KM (1991) Adsorption geometry and saturation coverage of Na on Si(100)2x1 surface: first principles calculations. Phys. Rev. B **44**, 8210-8213.

Editor's Note: All of the reviewer's concerns were appropriately addressed by text changes, hence there is no **Discussion with Reviewers**.